

Electric and Magnetic Field Control of Multiferroics Imaged with X-rays

Des McMorro
University College London

Outline

- Magneto-electric multiferroics
- TbMnO_3 : ferroelectricity induced by non-collinear magnetic order
- Non-resonant X-ray magnetic scattering (NRXMS)
- Electric field control of magnetic domains in TbMnO_3
- Towards imaging domains in multiferroic $\text{Ni}_3\text{V}_2\text{O}_8$

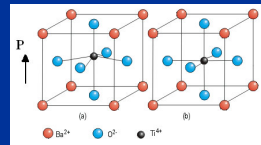
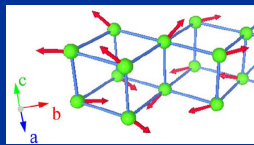
Multiferroics

- **Ferroc properties** : Spontaneous long-range order below a characteristic temperature
 - Presence of domains
 - Switch of the polarisation **P** by an applied electric field
 - Switch of the magnetisation **M** by an applied magnetic field
- **Multiferroics** : coexistence of two or more of the primary ferroic properties in the same phase

Magnetic order parameter

+

Electric order parameter



Magneto-electric Coupling

Application of electric and magnetic fields

Free energy:

$$F(\vec{E}, \vec{H}) = F_0 - P_i^S E_i - M_i^S H_i - \frac{1}{2} \epsilon_0 \epsilon_{ij} E_i E_j - \frac{1}{2} \mu_0 \mu_{ij} H_i H_j - \alpha_{ij} E_i H_j$$

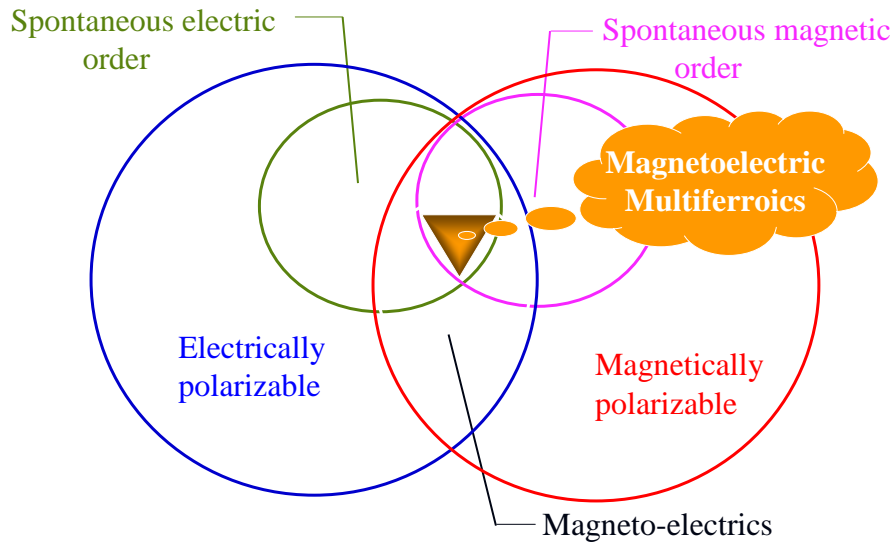
$$P_i(\vec{E}, \vec{H}) = -\frac{\partial F}{\partial E_i} = P_i^S + \epsilon_0 \epsilon_{ij} E_j + \alpha_{ij} H_j$$

$$M_i(\vec{E}, \vec{H}) = -\frac{\partial F}{\partial H_i} = M_i^S + \mu_0 \mu_{ij} H_j + \alpha_{ij} E_j$$

Induction of *electric* polarisation by a *magnetic* field and *magnetic* polarisation by an *electric* field

linear magnetoelectric effect

Magneto-electric Multiferroics

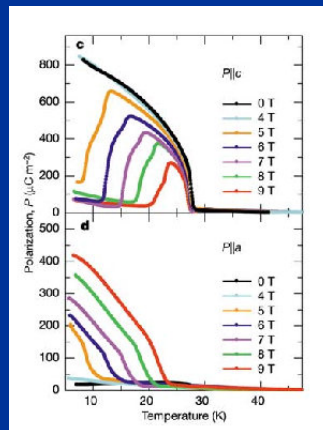
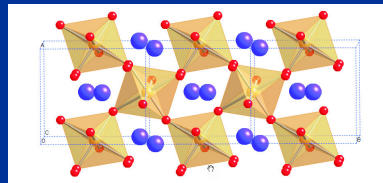
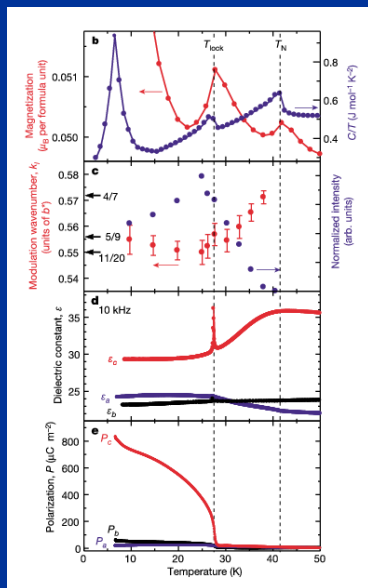


Magnetic Control of Ferroelectric Polarization

TbMnO₃

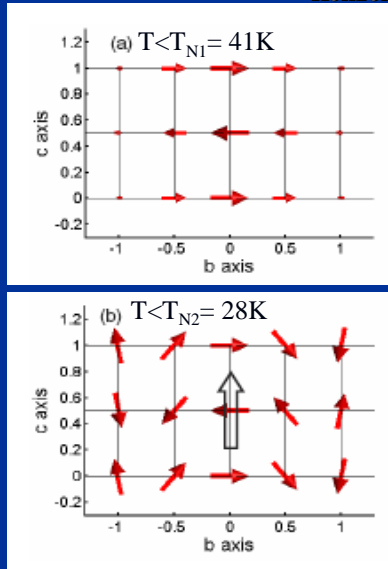
Kimura et al. Nature (2004)

Pbmn
Mn: bar 1
Tb: m



Magnetic inversion symmetry breaking and ferroelectricity in TbMnO₃

Kenzelmann et al. PRL (2005)



Neutron Scattering

$q_{Mn} = (0 \ q \ 1)$ A-type Fourier components

$$\Gamma_3: m_3[\text{Mn}] = (0.0 \ 2.9 \ 0.0)\mu_B$$

$$m_3[\text{Tb}] = (0.0 \ 0.0 \ 0.0)\mu_B$$

$$\Gamma_3: m_3[\text{Mn}] = (0 \ 3.9 \ 0)\mu_B \quad \Gamma_2: m_2[\text{Mn}] = (0 \ 0 \ 2.8)\mu_B$$

$$m_3[\text{Tb}] = (0 \ 0 \ 0)\mu_B$$

$$m_2[\text{Tb}] = (1.2 \ 0 \ 0)\mu_B$$

Phase between b and c components
not fixed by experiment

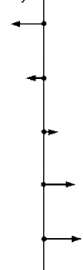
Ferroelectricity from Frustration!

Magnetically induced Ferroelectricity

Collinear

$$P = 0, C = 0$$

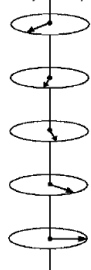
$$e_{ij} \uparrow (S_i \times S_j) = 0$$



Helical

$$P = 0, C = \uparrow$$

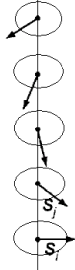
$$e_{ij} \uparrow (S_i \times S_j)$$



Cycloidal

$$P = \rightarrow, C = \odot$$

$$e_{ij} \uparrow \odot (S_i \times S_j)$$



Magnetic "chirality" C :

$$C \propto \sum_i S_i \times S_{i+1}$$

Electric polarisation P :

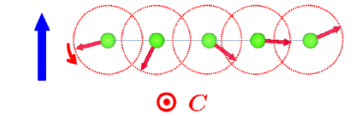
$$P \propto \sum_i e_{i,i+1} \times (S_i \times S_{i+1})$$

- Inverse Dzyaloshinskii–Moria Interaction
Mostovoy, *PRL* (2006); Sergienko, *PRB* (2006).
- Spin current
Katsura, Nagaosa, Balatsky, *PRL* (2005).

"Chirality" and Ferroelectric domains :

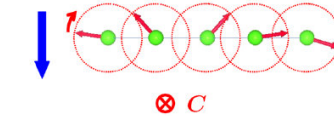
Counterclockwise:

$$P_c > 0$$



Clockwise:

$$P_c < 0$$



X-ray Magnetic Scattering

(1972) X-ray Magnetic Scattering

(1985) First Resonant Scattering

Nickel, Namikawa (1985)

Copyrighted image

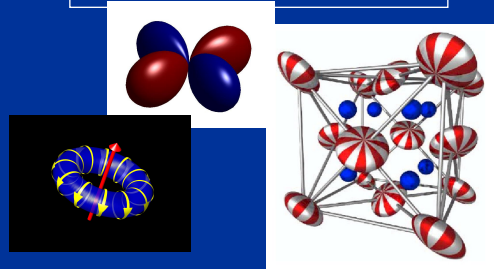
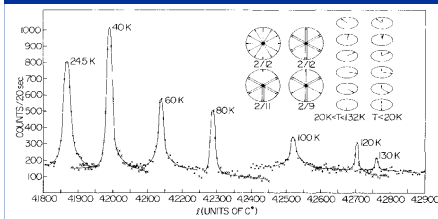
Copyrighted image

NiO, de Bergevin and Brunel (1972)

(1985) First Synchrotron Studies

Holmium, Gibbs et al. (1985)

"Modern" Era?!



NRXMS cross-section

$$f(\mathbf{K}) \propto \sum_j \exp(i\mathbf{K} \cdot \mathbf{r}_j) (\mathbf{S}_j \cdot \mathbf{B} + \frac{1}{2} \mathbf{L}_j \cdot \mathbf{A}'')$$

Structure factor

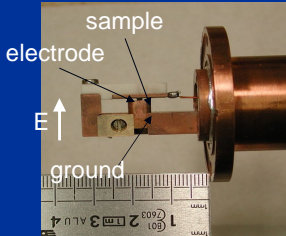
Scattering wave-vector
 $\mathbf{K} = \mathbf{k} - \mathbf{k}'$

FT of Spin and orbital densities

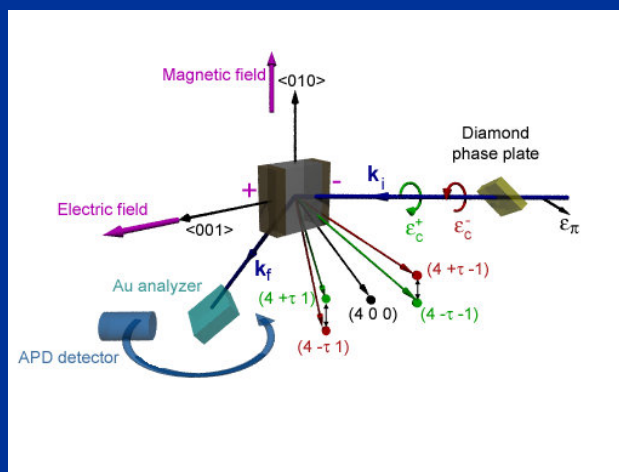
Polarisation factors of incident and scattered beam


Geometrically coupled

Diffraction in E&H fields on ID20, ESRF



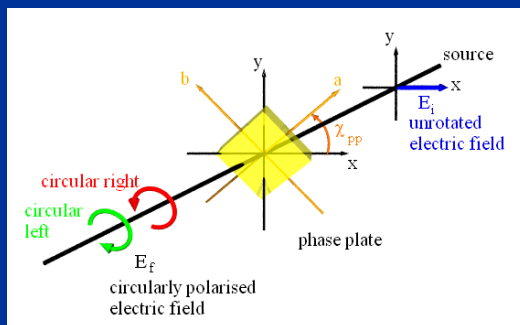
sample
electrode
ground



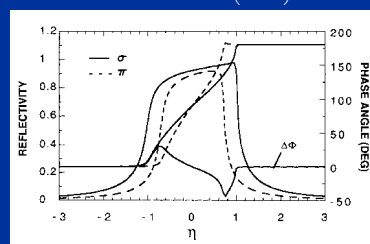


Production of circularly polarized X-rays

- Perfect diamond crystals can act as $\lambda/4$ plate producing circularly polarised light



Batterman PRB (1992)

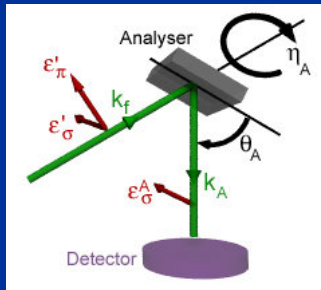


$\epsilon=7.5$ keV: diamond thickness = 1200 μm , Circular polarisation ~ 98%

$\epsilon=6.15$ keV: diamond thickness = 700 μm , Circular polarisation ~ 99%

- Handedness of circularly polarised light couples to handedness of chiral spin structures

Polarization analysis of the scattered beam

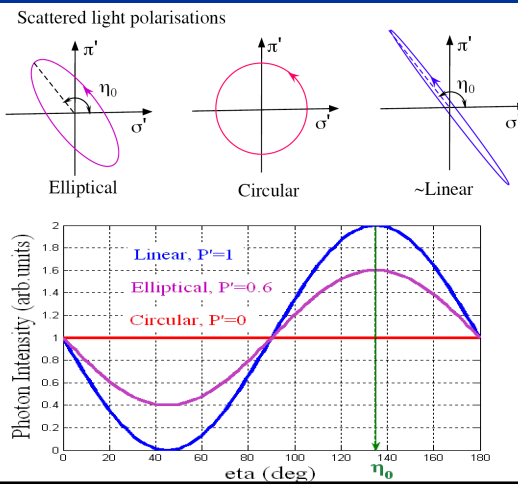
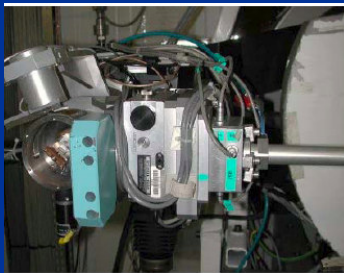


Beam polarization characterised by Stokes Parameters

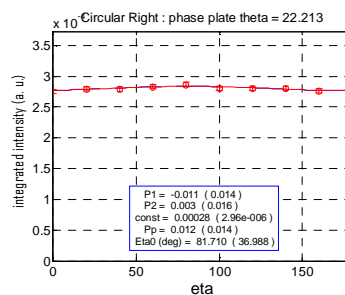
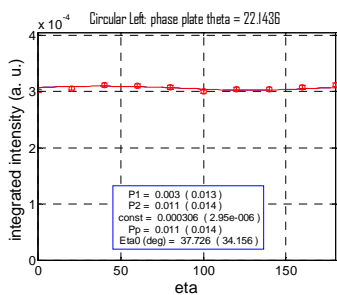
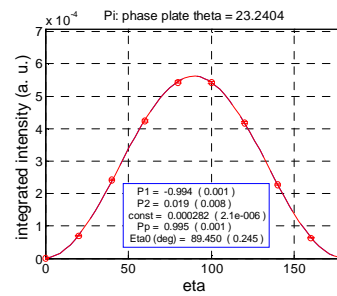
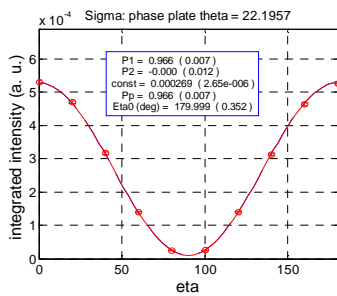
$$(P_1, P_2, P_3)$$

Experiment determines linear parameters P_1 and P_2

$$I(\eta) = 1 + P_1 \cos(2\eta) + P_2 \sin(2\eta) = 1 + P' \cos(2(\eta - \eta_0))$$



Stokes Parameters of Direct Beam

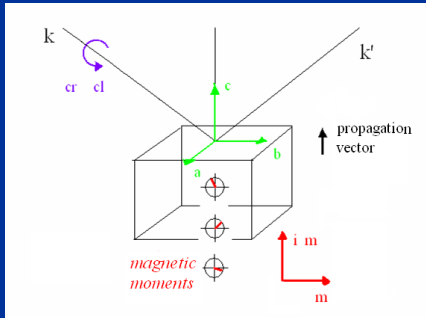


Circularly polarized light and cycloidal domains

LINEAR LIGHT : Same scattering cross-section for the two cycloidal domains

CIRCULAR LIGHT : Coupling between chirality of the magnetic structure and handedness of the circular light \rightarrow possible to discriminate

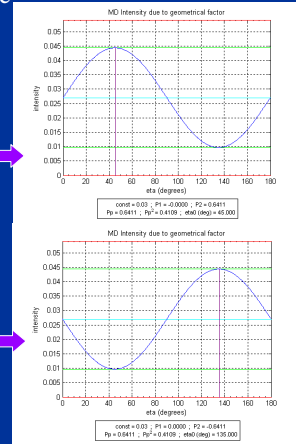
ex. : simple magnetic structure ; non resonant scattering



circular right,
monochiral
domain

$$\eta_0 \rightarrow \eta_0 + 90^\circ$$

circular left,
monochiral
domain

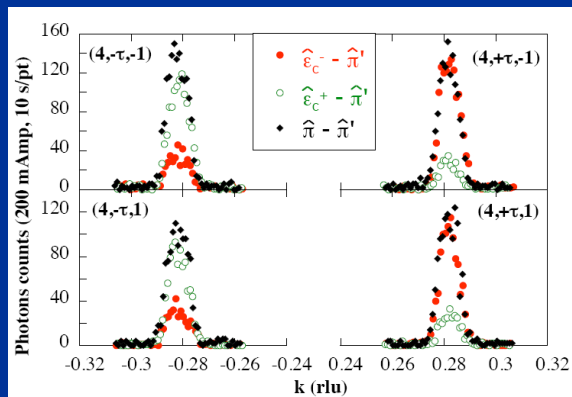


Reversing the circular polarisation \equiv exchanging domains

Dependence of NRXMS on incident polarization

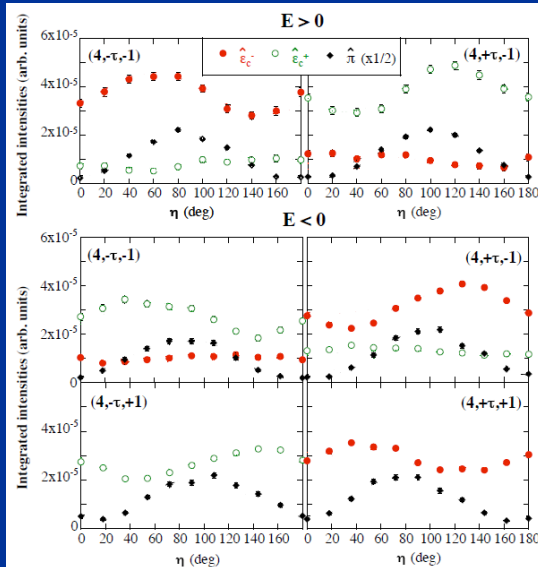
Electric Field Cooling

- $T=15$ K i.e. in FE phase, field cooling -700 V
- $E=7.5$ keV
- A-type star of wave-vectors
- Measured in π' channel



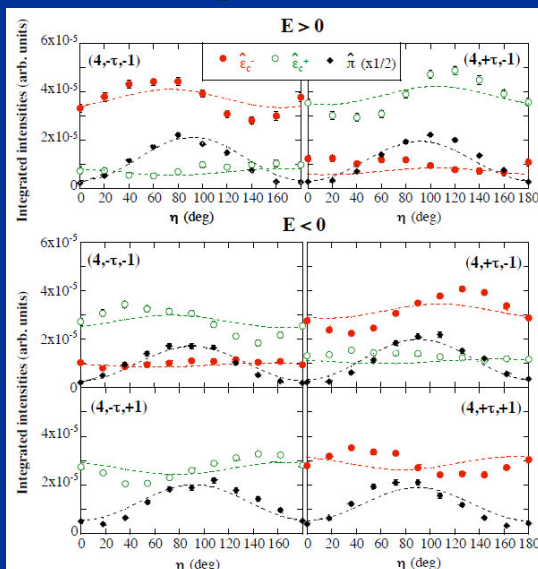
- All 4 intensities similar for $\pi-\pi'$
- $I(\epsilon_c^- - \pi') \neq I(\epsilon_c^+ - \pi')$, complementary behaviour depending on $\pm\tau$
- Demonstrates imbalance of cycloidal domains

Switching of Cycloidal domains by an E field



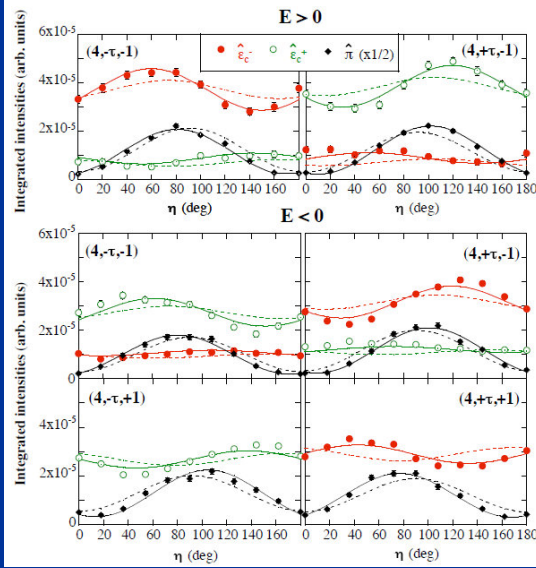
- π - incident little difference in $|I(\eta)|$, but symmetries in $I(\eta) = I_{\max}$ for $\pm\tau \pm 1$
- Big differences in $I(\eta)$ for $\hat{\epsilon}_c^-$ and $\hat{\epsilon}_c^+$
- Behaviour reversed by electric field direction, ie E-field switching of domain populations

Comparison with Kenzelmann model



- Dashed lines for Kenzelmann model – IC structure with cycloidal ordering of Mn spins rotating in bc plane + Tb moment along a
- Unsatisfactory agreement with data

New magnetic structure model



- Additional Tb spin moment component along b
- Plus Tb orbital moment equal in size to spin component
- Phase relationships fixed between different components of magnetization

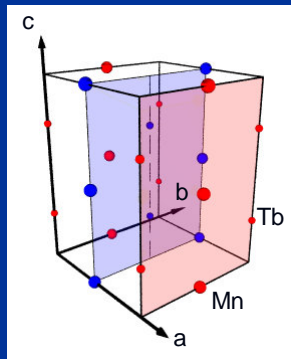
Modelling NRXMS from TbMnO₃

$$f(\mathbf{K}) \propto (S_b^M(\mathbf{K})\hat{\mathbf{b}} - \gamma \alpha i S_c^M(\mathbf{K})\hat{\mathbf{c}}) \cdot \mathbf{B} \\ - \gamma \beta i (S_b^T(\mathbf{K})\hat{\mathbf{b}} \cdot \mathbf{B} + \frac{1}{2} L_b^T(\mathbf{K})\hat{\mathbf{b}} \cdot \mathbf{A}^n) \cos(8\pi\Delta_a^T)$$

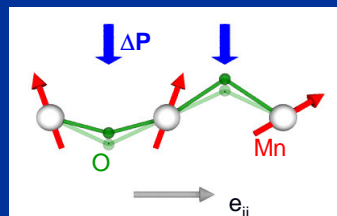
where the value of $\alpha = \pm 1$ selects the sign of τ , β the sign of $l = \pm 1$ and $\gamma = \pm 1$ identifies the two chiral domains 1 and 2, respectively (Fig. 4(b)). The vectors \mathbf{A}^n and \mathbf{B} contain the dependence on the polarization of the incident and diffracted light¹⁶. The spin $S_i(\mathbf{K})$ and the orbital $L_i(\mathbf{K})$

$$f_{\hat{\sigma}^i} \propto S_b^M + \epsilon \alpha \gamma S_c^M - i \beta \gamma S_b^T \\ f_{\hat{\pi}^i} \propto (\epsilon \beta \gamma)(S_b^T + L_b^T) + i(\epsilon S_b^M + \alpha \gamma S_c^M)$$

Proposed magnetic structure - Mn

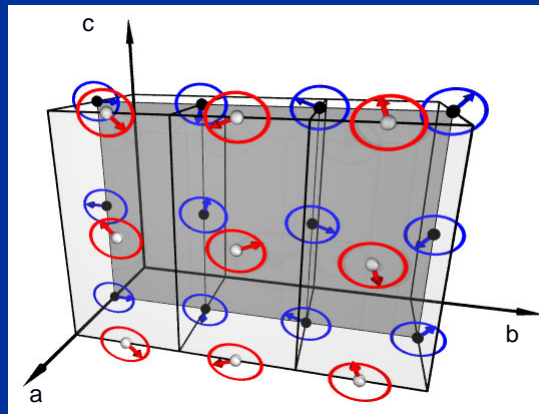


IDMI



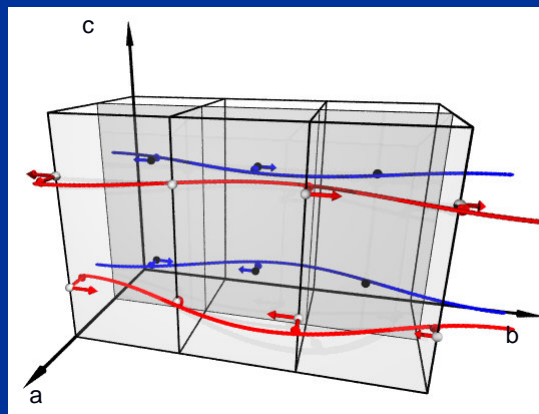
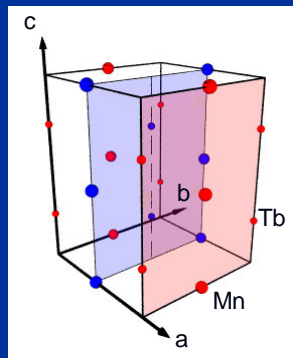
- Cycloid in bc plane with:

$$m_{\Gamma_2} = (0, 0, 2.8)\mu_B, m_{\Gamma_3} = (0, 3.9, 0)\mu_B$$

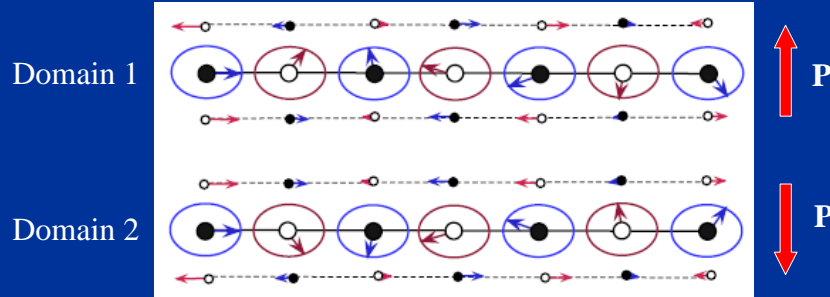


New magnetic structure of Tb sublattice

- 2 orbits unrelated by symmetry. Moments sinusoidally modulated with both longitudinal and transverse components

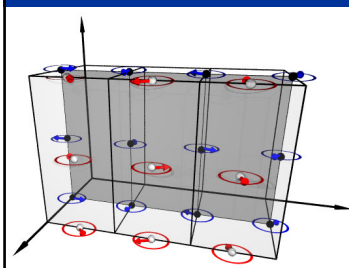
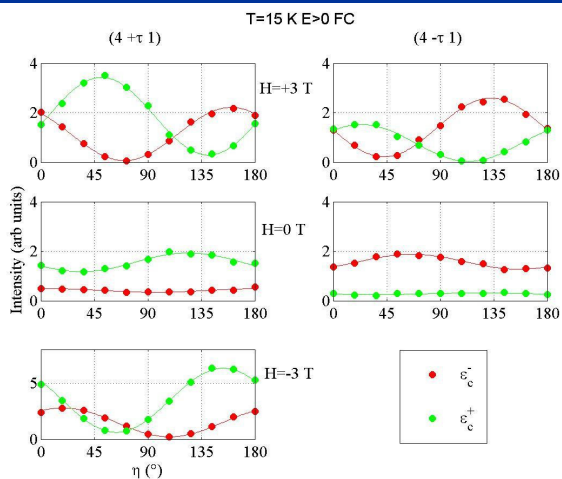
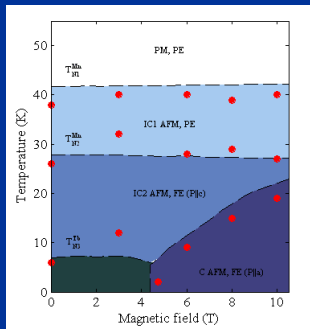


Electric Field Control of Cycloidal domains



- Projection of domains in bc plane with newly determined longitudinal component of Tb moment
- $E > 0$ field cooling $\rightarrow 96 \pm 3\%$ Domain 1
- $E < 0$ field cooling $\rightarrow 93 \pm 2\%$ Domain 2
- Absolute measurement of sense of rotation (chirality)
- Fabrizi et al., PRL 2009

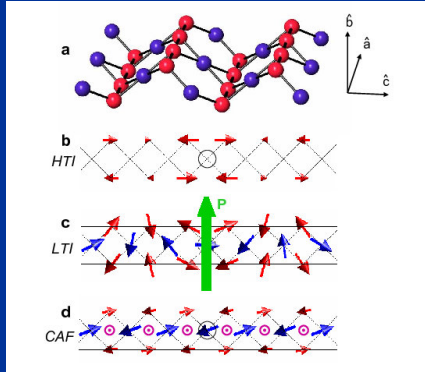
Magnetic field induced polarisation flop



Work in progress....

Multiferroicity on a Kagome Staircase: $\text{Ni}_3\text{V}_2\text{O}_8$

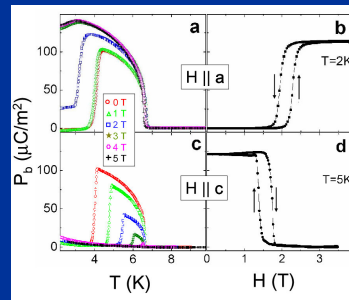
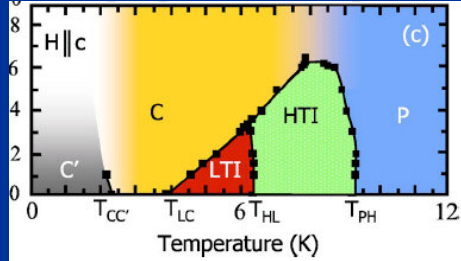
Lawes et al., PRL: 93 247201 (2004); 95 087205 (2005)



Neutron diffraction: $\tau=[0.27\ 0\ 0]$

HTI: $m_4^S=(1.93\ 0\ 0)\ \mu_B$
 $m_4^C=(0\ 0\ 0)\ \mu_B$

LTI: $m_4^S=(1.6\ 0\ 0)\ \mu_B$
 $m_1^S=(0\ 1.3\ 0)\ \mu_B$
 $m_4^C=(0\ 1.4\ 0)\ \mu_B$
 $m_1^C=(-2.2\ 0\ 0)\ \mu_B$



Electric field control of magnetic domains in $\text{Ni}_3\text{V}_2\text{O}_8$

Spines, LTI Phase

Spines:

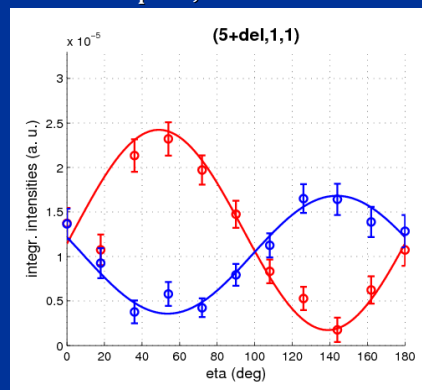
$h=\text{odd}, k=\text{odd}, l=\text{odd}$

Cross ties:

$h=\text{even}, k=\text{even}, l=\text{odd}$

Spines+ Cross ties:

$h=\text{odd}, k=\text{odd}, l=\text{even}$



- Beam heating => attenuate incident beam by a factor of 100
- 10^{13} photons in, 10^0 out
- Two parameter fit:

Scale factor

Domain population of 88(3) %

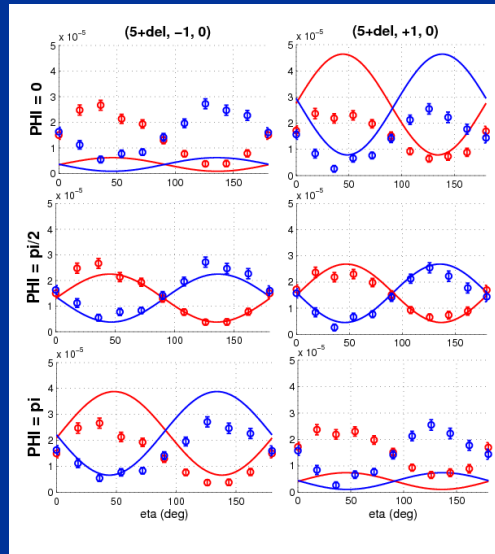
Electric field control of magnetic domains in $\text{Ni}_3\text{V}_2\text{O}_8$

Spines+Cross ties, LTI Phase

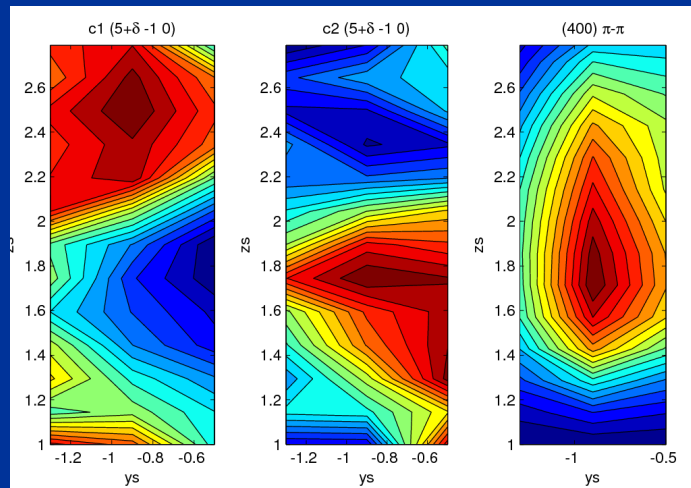
- Phase shift between Spines and cross ties undetermined from neutron diffraction
- NRXMS gives best fit of $\pi/2$
- Systematic behaviour consistent with analytical approximation of structure factor:

$$\text{Intensities} \Rightarrow \phi = \pi/2$$

$$P_1=0 \Rightarrow m_a/m_b=1$$
- Inconsistent with neutron diffraction which yields $m_a/m_b=1.5$



Imaging Cycloidal Domains in $\text{Ni}_3\text{V}_2\text{O}_8$



Conclusions

- Non-resonant Magnetic Scattering
 - Demonstration of electric control of magnetic domain population
 - Combination of circular light and full polarimetry: new technique for studying non-collinear magnetic structures
 - Potential wide spread application to multiferroics and other materials

Acknowledgements

- Francois de Bergevin ESRF
- Andrew Boothroyd Oxford
- **Federica Fabrizi** UCL/ESRF
- Michel Kenzelmann PSI
- Luigi Paolosini ESRF
- Dharmalingam Prabhakaran Oxford
- **Helen Walker** UCL/ESRF

- **Beamline ID20**